Structure of TIGIT immunoreceptor bound to poliovirus receptor reveals a cell–cell adhesion and signaling mechanism that requires *cis-trans* receptor clustering

Katharina F. Stengel[a,b], Kristin Harden-Bowles[c], Xin Yu[d], Lionel Rouge[a], Jianping Yin[a], Laëtitia Comps-Agrar[c], Christian Wiesmann[a,1], J. Fernando Bazan[a,b,2], Dan L. Eaton[c], and Jane L. Grogan[d,3]

[a]Department of Structural Biology, [b]Department of Early Discovery Biochemistry, [c]Department of Protein Chemistry, and [d]Department of Immunology Research, Genentech, Inc., South San Francisco, CA 94080

Edited by Lewis L. Lanier, University of California, San Francisco, CA, and approved February 14, 2012 (received for review December 14, 2011)

Nectins (nectin1–4) and Necls [nectin-like (Necl1–5)] are Ig superfamily cell adhesion molecules that regulate cell differentiation and tissue morphogenesis. Adherens junction formation and subsequent cell–cell signaling is initiated by the assembly of higher-order receptor clusters of cognate molecules on juxtaposed cells. However, the structural and mechanistic details of signaling cluster formation remain unclear. Here, we report the crystal structure of poliovirus receptor (PVR)/Nectin-like-5/CD155) in complex with its cognate immunoreceptor ligand T-cell-Ig-and-ITIM-domain (TIGIT). The TIGIT/PVR interface reveals a conserved specific "lock-and-key" interaction. Notably, two TIGIT/PVR dimers assemble into a heterotetramer with a core TIGIT/TIGIT *cis*-homodimer, each TIGIT molecule binding one PVR molecule. Structure-guided mutations that disrupt the TIGIT/TIGIT interface limit both TIGIT/PVR-mediated cell adhesion and TIGIT-induced PVR phosphorylation in primary dendritic cells. Our data suggest a *cis-trans* receptor clustering mechanism for cell adhesion and signaling by the TIGIT/PVR complex and provide structural insights into how the PVR family of immunoregulators function.

Nectins (nectin1–4) and nectin-like (Necl1–5) molecules are members of the large Ig superfamily (IgSF) of cell-surface receptors that play central roles in cell adhesion, cell movement, proliferation, and survival and contribute to the morphogenesis and differentiation of many cell and tissue types by inducing an intracellular signaling cascade (1–5). Nectins and Necls can function as both ligands and receptors and therefore are able to signal bidirectionally into juxtaposed cells (3, 6). To mediate the formation of cell adherens junctions, a model suggests that the extracellular domains of these molecules form ligand-dependent homo- or heterodimers in *trans* (between molecules located on the same or opposite cell surfaces, respectively) and lateral homodimers in *cis*, creating a tight network of nectin zippers between juxtaposed cells (7, 8). To date, structural and functional studies suggest a mechanism whereby the *cis*-homodimerization of a receptor on the same cell surface is followed by the formation of a *trans*-dimer between juxtaposed cells using identical protein interfaces. This assembly is noteworthy because it requires a rearrangement and breakup of the *cis*-homodimer followed by a *trans*-dimerization across the adherens junction. The *cis-trans* clustering is then initiated through another unknown protein interface, likely involving a different receptor domain.

Several high-affinity homophilic *trans*-interactions have been described in detail for nectins/Necls and similar molecules (8–13). However, the structure and function of the presumably weaker lateral homophilic *cis*-dimers in cell adhesion and their role in intracellular signaling is not known. Because all structures solved to date are homodimers, it is unclear if they represent the *cis*- or the *trans*-state. Thus, the question of how *cis-trans* heterodimerization drives cell adhesion and intracellular signaling remains open and was the impetus for capturing the heterophilic interaction of the poliovirus receptor (PVR; also known as CD155 or Necl–5) (14) with its high-affinity ligand TIGIT (T-cell-Ig-and-ITIM domain) (4, 15, 16).

PVR, a prototypical Nectin/Necl family member, is notable among the nectin/Necl family as it not only provides heterophilic interactions with other nectin family members, such as nectin-3 (17, 18), but also it interacts with IgSF molecules on immune lymphocytes such as TIGIT, CD226 (also known as DNAM-1) (19), and CD96 (20) to regulate immune responses (21). Ligation of PVR induces tyrosine phosphorylation of the PVR immunoreceptor tyrosine-based inhibitory motif (ITIM) domain and recruitment of Src kinases and SHP-2 (SH2-domain-containing tyrosine phosphatase-2) (2, 4, 22–24). Activation of PVR with TIGIT has been shown to attenuate immune responses in vivo, predominantly through activation and phosphorylation of Erk and induction of the suppressive cytokine IL-10 from dendritic cells (4). Originally, PVR was classified as a nectin-like molecule (Necl–5) largely on the basis of a shared intracellular motif; however, sequence analysis suggests that PVR is more similar to the nectins (4). Recently, we identified PVR family signature sequences in the IgSF ectodomains of PVR, nectins, TIGIT, CD226, and CD96 (4). Despite being diverse in domain architecture, all PVR family members share three unique and highly conserved sequence motifs in the first immunoglobulin variable (IgV) domain: the (V/I)(S/T)Q, AX_6G, and T(F/Y)P motifs (4). Like other nectins, PVR can form homodimers and multimers in *cis* on cells (1, 17).

Here we present the crystal structures of TIGIT alone and in complex with PVR. The 2.9-Å resolution structure of TIGIT in complex with PVR reveals a distinct "lock-and-key" motif that is highly conserved across the PVR family members and is critical for the TIGIT–PVR binding. Notably, the structure revealed a heterotetrameric assembly of two TIGIT molecules flanked by two PVR molecules. We show that the core TIGIT/TIGIT interface is distinct from the PVR/TIGIT interface and can exist in preformed lateral *cis*-dimers at the cell surface. Disruption of these TIGIT dimers, by site-directed mutagenesis, impaired cell adhesion to and signaling in PVR-expressing cell lines and primary human dendritic cells (DCs). Our data show that the lateral TIGIT homodimers, together with the *trans*-TIGIT/PVR heterodimers,

Author contributions: K.F.S., C.W., J.F.B., D.L.E., and J.L.G. designed research; K.F.S., K.H.-B., X.Y., L.R., J.Y., and L.C.-A. performed research; K.F.S., K.H.-B., X.Y., L.R., L.C.-A., C.W., J.F.B., D.L.E., and J.L.G. analyzed data; and K.F.S., J.F.B., and J.L.G. wrote the paper.

Conflict of interest statement: During these studies, all authors were employed by Genentech, Inc., which develops and markets drugs for profit.

This article is a PNAS Direct Submission.

Data deposition: Crystallography, atomic coordinates, and structure factors reported in this paper have been deposited in the Protein Data Bank, www.pdb.org (PDB ID codes 3UCR and 3UDW).

[1]Present address: Novartis, 4002 Basel, Switzerland.

[2]Present address: NeuroScience, Osceola, WI, 54020.

[3]To whom correspondence should be addressed. E-mail: jgrogan@gene.com.

This article contains supporting information online at www.pnas.org/lookup/suppl/doi:10.1073/pnas.1120606109/-/DCSupplemental.

can oligomerize in a zipper-like fashion to facilitate adhesion of adjacent immune cells and thereby form receptor clusters that are required for effective activation of PVR signaling.

Results

Crystal Structures of TIGIT and TIGIT Bound to PVR. To understand the molecular mechanism of the TIGIT/PVR *trans*-dimerization, we determined the crystal structures of TIGIT and TIGIT bound to PVR. Our work and previous experiments have shown that the N-terminal IgV domain of human PVR (PVR D1) is important for TIGIT IgV binding (4). Human TIGIT IgV was expressed in *Escherichia coli* and purified from inclusion bodies. Similarly, human PVR D1 domain was expressed in the insect cell-baculovirus system, purified, and complexed with TIGIT IgV. This complex was stable and showed that TIGIT IgV and PVR D1 are necessary and sufficient for TIGIT/PVR complex formation (Fig. S1). We crystallized TIGIT alone and TIGIT in complex with PVR and solved the structures at 2.7 and 2.9 Å resolution, respectively (Table S1 and Fig. 1).

The TIGIT IgV domain and PVR D1 have a typical and very similar Ig β-sandwich fold (Fig. S2) that is also very similar to that of Necl-1 (Fig. S3*A*). The canonical A strand is composed of A and A′ halves shared between the two β-sheets. The PVR-family submotifs (V/I)(S/T)Q, AX_6G, and T(Y/F)P are mapped to strands C, C′, and F (Fig. S3*B*) (4).

In contrast to canonical Ig-domain family members, the C′C″ and FG loops have insertions of four and two residues, respectively (Figs. S2 and S3). Furthermore, the loop connecting strands D and E (DE loop) in TIGIT is shortened by four residues in comparison with Necl-1 and is kinked by two proline residues (P80 and P82) (Figs. S2*A* and S3). Unlike TIGIT, PVR has an unusually elongated DE loop (Figs. S2*B* and S3) compared with other nectins/Necls (11). Carbohydrate moieties from the insect cell expression system are present on both predicted

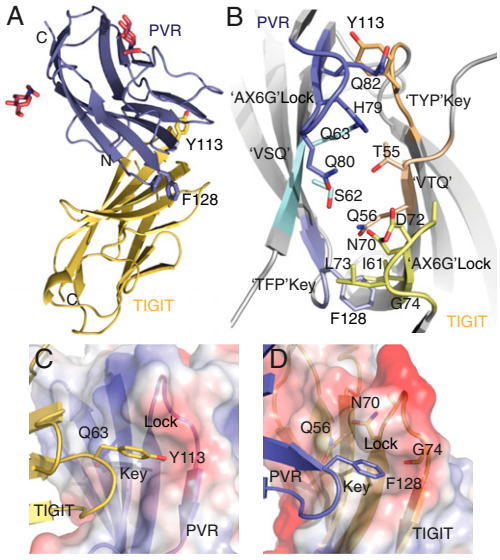

Fig. 1. Structure of the TIGIT/PVR complex. (*A*) Side view of the TIGIT IgV domain (gold) in complex with the PVR D1 domain (blue; sugar moieties in red). The TIGIT/PVR interface shows a conserved lock-and-key (*B*) interaction between the two molecules. The "lock" is formed by the AX_6G motif, and the "key" is formed by the corresponding T(Y/F)P motif on the neighboring molecule. The "key" residues Tyr113 and Phe128 in the conserved TIGIT motif TYP and the PVR motif TFP are labeled. Both (V/I)(S/T)Q motifs are also located in the complex interface. (*C*) Detailed view of the "key" formed by Tyr113 in TIGIT and the lock formed by the AX_6G motif of PVR. (*D*) Detailed view of the "key" formed by Phe128 on PVR and of the lock formed by the AX_6G motif of TIGIT.

N-linked glycosylation sites of PVR (N105 and N120) and located on each β-sheet of the IgV domain without interfering with TIGIT binding. TIGIT lacked carbohydrate modifications, as it was expressed in *E. coli*, but neither of the two potential glycosylation sites (TIGIT residues N32 and N101) is close to the PVR-binding site. Neither TIGIT nor PVR showed significant conformational rearrangements upon complex formation (TIGIT rmsd of 0.8 Å over 105 Cα residues, PVR RMSD of 1.88 Å over 103 Cα atoms). The crystal structures confirm that, despite low sequence homology, both PVR and TIGIT IgV domains are very similar to each other and so they are grouped in the PVR family of cell adhesion molecules (4).

TIGIT/PVR Interface Contains Lock-and-Key Binding Pockets. In the TIGIT/PVR *trans*-dimer complex structure, the TIGIT/PVR interface is formed by interactions between the front β-sheets (A′GFCC′C″) of each molecule (Fig. 1 and Fig. S4*A*). Because receptor and ligand share the same IgV fold, the interface displays approximate noncrystallographic twofold symmetry and is highly complementary in shape and charge. Interestingly, the interface in the TIGIT/PVR complex uses the same structural elements as other IgV homo- and heterodimers (Fig. S4 *A*–*G*). A similar interaction for homodimerization is also observed for PVR alone (11) (Fig. S4*C*) and in the TIGIT crystal structure (Fig. S4*B*).

In the TIGIT/PVR *trans*-dimer, the FG loop of each IgV domain contacts the C′C″ loop of its partner (Fig. 1*A*). The interfaces bury a total molecular surface area of about 1,600 $Å^2$. Additionally, the conserved sequence motifs AX_6G (residues 76–83 in PVR, 66–74 in TIGIT) in the C′C″ loop and T(F/Y)P in the FG loop (residues 127–129 in PVR and residues 112–114 in TIGIT) define signature lock-and-key interactions on symmetric corners of the interface that literally latch the two molecules together (Fig. 1 *B*–*D*). The concave "lock" on each molecule is formed by the conserved AXXXXXZG (AX_6G) motif in the C′C″ loop that creates a hydrophobic pocket with the Z residue as a lid. The convex "key" feature consists of a conserved aromatic residue in the FG loop (Y113 in TIGIT and F128 in PVR) that latches into the hydrophobic lock pocket on the opposing molecule (Fig. 1 *C* and *D*). These lock-and-key motifs are highly conserved in the IgV domain of nectins but not Necls and comprise the distinctive PVR family motifs (Fig. S3*B*) (4). Together with a third (V/I)(S/T)Q pattern (residues 54–56 on TIGIT, 61–63 on PVR) that also contributes to the intermolecular packing in the TIGIT/PVR complex, these structural motifs account for most of the TIGIT/PVR interaction topography (Fig. 1 *B*–*D*). Interestingly, mapping of mutants that affect the PVR–poliovirus interaction (11) onto the TIGIT/PVR structure reveals that both poliovirus and TIGIT use the same surface and residues on PVR for binding (Fig. S3*C*). This overlap of ligand and virus binding sites also has been reported for other virus receptors (9, 25).

Mutational Analysis at the TIGIT/PVR Lock-and-Key Interface. To investigate the importance of the conserved PVR motifs for the lock-and-key complex formation, a number of point mutants in the PVR motifs of TIGIT and PVR were created (Fig. 1*B*). Each mutant protein was cloned as an Fc-fusion protein, expressed and purified from CHO cells, and binding was determined using biolayer interferometry (BLI) and flow cytometry binding assays. As previously reported, wild-type PVR and wild-type TIGIT proteins interacted strongly in *trans* with each other (Fig. 2) (4). TIGIT point mutants Q56A and Q56R in the (V/I)(S/T)Q motif, N70R, N70A, G74A in AX_6G, and Y113R and Y113A in the T(F/Y)P region weaken or abrogate binding to PVR (Fig. 2*A*). The mutation of the "key" aromatic residue on TIGIT (Y113) weakened but did not disrupt the *trans*-TIGIT/PVR interaction. Reciprocally, all PVR point mutants—Q63R, Q63A in the (V/I)(S/T)Q motif, and the "key" region variants F128R and F128A in the T(F/Y)P motif—reduce or abrogate binding to TIGIT (Fig. 2*B*). The BLI data

were complemented by the ability of the various Fc-fusion proteins to bind cell lines stably expressing TIGIT or PVR on the cell surface, showing more subtle effects on the TIGIT side from weakening the interaction until blockage occurs (Q56R and N70R) (Fig. 2*C*) and strong effects with the PVR point mutations up to a complete loss of interaction (Q63R, F128R, F128A) (Fig. 2*D*). Taken together, we conclude that the lock-and-key *trans*-interactions between TIGIT and PVR are the main interaction points and critically require the "key" motif T(F/Y)P on both PVR and TIGIT for *trans*-complex formation.

TIGIT/PVR Complex Forms a Tetramer in the Crystal Structure. The TIGIT/PVR complex crystallized in the space group $P3_221$, with two TIGIT and two PVR molecules in the asymmetric unit. Surprisingly, crystal packing generates a heterotetrameric assembly of the two TIGIT and two PVR molecules in the shape of a symmetrical double-winged structure (Fig. 3*A*). An identical homotetramer created by crystal packing is observed for TIGIT alone (Fig. 3*B* and Protein Data Base ID 3Q0H and 3RQ3). The core of the TIGIT/PVR heterotetramer and the TIGIT homotetramer is formed by a symmetrical homodimer of two TIGIT molecules in which the C termini are in close proximity to each other (Fig. 3 *A* and *B*), allowing for the formation of a TIGIT lateral *cis*-homodimer on cells. A similar crystal packing has also been described for Nectin-1 in complex with glycoprotein D from herpes simplex virus (9). The interface of this TIGIT homodimer buries a total molecular surface area of about 1,000 Å^2 and uses the flat surface of the four-stranded β-sheet on the back of the molecule (Fig. 3*B*). Each monomer packs tightly against its counterpart and is held together by main-chain interactions and

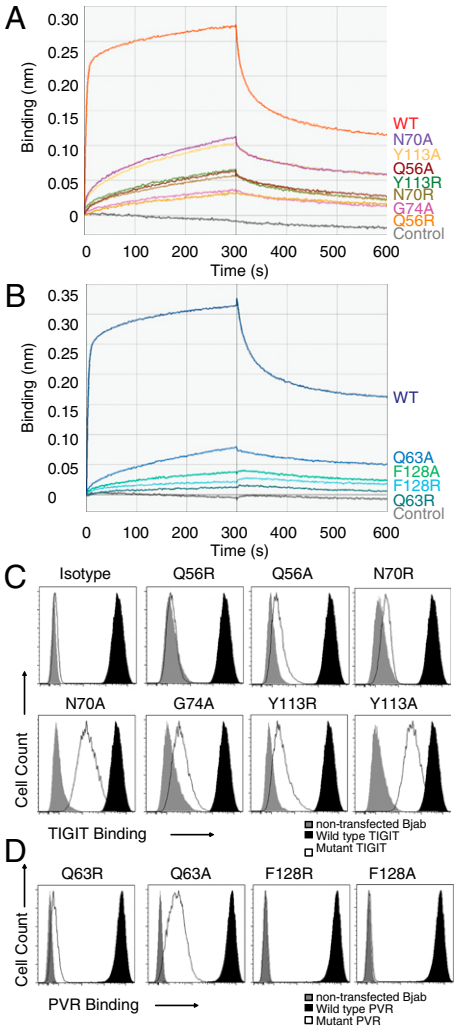

Fig. 2. The lock-and-key motif is necessary for TIGIT/PVR complex formation. (*A*) BLI sensograms of the binding of PVR-Fc WT to TIGIT-Fc WT or TIGIT-Fc single point mutants immobilized on anti-human Fc biosensors; data are representative of two experiments. (*B*) BLI sensograms of the binding of PVR-Fc WT or PVR-Fc single point mutants to TIGIT-Fc WT immobilized on anti-human Fc biosensors; data are representative of two experiments. (*C*) Flow cytometry analyses of TIGIT-Fc WT or TIGIT-Fc single point mutants binding to BJAB cells stably expressing PVR. The gray-shaded histogram represents binding to nontransfected BJAB cells; the black-shaded histogram represents binding of WT TIGIT-Fc; the unfilled histogram represents the binding of the indicated point mutant. (*D*) Flow cytometry analysis of PVR-Fc WT or PVR-Fc point mutants binding to BJAB cells stably expressing TIGIT; data are representative of two experiments. The gray-shaded histogram represents binding to nontransfected BJAB cells; the black-shaded histogram represents binding of WT PVR-Fc; the unfilled histogram represents binding of the indicated point mutant.

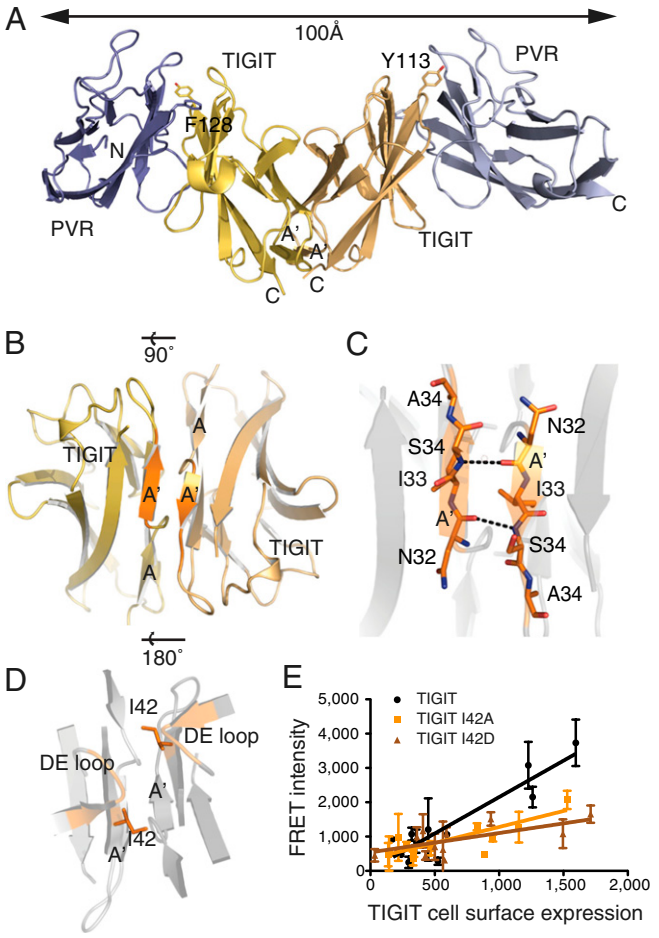

Fig. 3. Structure of the TIGIT/PVR complex reveals a heterotetrameric assembly with a TIGIT/TIGIT homodimer core. (*A*) A core TIGIT homodimer (gold) with proximal C termini is flanked by two PVR (blue) molecules. (*B*) Bottom view of the core TIGIT/TIGIT homodimer present in the TIGIT and TIGIT/PVR structures. (*C*) Detailed view of the symmetrical TIGIT/TIGIT homodimer interface, formed by main-chain interactions of the two A′ strands and (*D*) residue Ile42 as dimer core. (*E*) TR-FRET between ST-TIGIT receptors. FRET intensity was measured using SNAP-Lumi4-Tb (donor) and SNAP-A647 (acceptor) on COS7 cells expressing increasing amounts of ST-TIGIT (black), TIGIT I42A (orange), and TIGIT I42D (brown). FRET intensity is represented according to the cell-surface TIGIT expression as recorded by the donor emission. The signal recorded on mock cells was previously subtracted. Data represent triplicate determinations from two independent experiments.

a β-sheet extension of the six-stranded (A′GFCC′C″) β-sheet between the two molecules (Fig. 3 *B* and *C*). A core residue of this interface is Ile42, which binds into a groove formed by the main-chain atoms of Thr29 and Cys45 on the opposing TIGIT monomer (Fig. S4*H*). The split of the A strand into A and A′ halves structurally supports this dimerization interface. The two A′ β-strands of adjacent molecules zipper together in antiparallel fashion with a tight hydrogen-bonding network.

Because the TIGIT/TIGIT homodimer interface is unique and distinct from the lock-and-key *trans*-TIGIT/PVR interaction surface, we asked if the TIGIT/TIGIT homodimer was biologically meaningful and might stand as a distinct state (on the surface of the same cell) in contrast to the *trans*-TIGIT/PVR complex connecting two juxtaposed cells. To investigate the biological relevance of TIGIT/TIGIT homodimers, we set out to characterize the dimer interface. TIGIT IgV domain alone is monomeric and TIGIT/PVR is a dimer in solution (Fig. S1). However, the TIGIT IgV domain displayed a transformation from a monomeric to a multimeric species at high concentrations using gradient diffusion NMR at several concentrations (Fig. S5*A*) and was determined to have a high dissociation constant ($K_d > 1$ mM). Analytical ultracentrifugation experiments at a low concentration (200 μM) showed that TIGIT was mostly monomeric and undergoing concentration-dependent self-association, as evidenced by the 10% increase in sedimentation coefficient observed upon increasing the concentration (Fig. S5*B*). Pointedly, a similarly weak association has been reported for CAR-JAML *cis*-heterotetramer formation (25) and *cis*-oligomerization of cadherins (26, 27).

TIGIT Assembles as *cis*-Homodimers on the Surface of Cells. To investigate if these TIGIT homodimers or oligomers were present on the cell surface, TIGIT/TIGIT homodimer formation was analyzed on the cell surface by time-resolved Förster resonance energy transfer (TR-FRET). COS7 cells were transfected with increasing amounts of snap-tagged full-length TIGIT (ST-TIGIT) and double-labeled with a fixed concentration of FRET donor and acceptor (Fig. S6). A significant TR-FRET signal was detected with the ST-TIGIT, indicating that TIGIT can form *cis*-homodimers or multimers on the surface of cells (Fig. 3*E*), although we cannot quantitate the proportion of monomers to homodimers or oligomers with this technique. In the FRET experiments, separate batches of COS7 cells were transfected with an increasing amount of TIGIT, and the FRET resonance remained linear rather than exponential. Structure-guided point mutations of the core residue (Ile42) in the TIGIT homodimer interface, I42A and I42D, showed a reduced TR-FRET signal. This indicates that the I42A and I42D point mutants destabilize TIGIT *cis*-homodimerization on the surface of cells. Taken together, the data support the ability of TIGIT to form lateral *cis*-homodimers on the cell surface of these transfected cells.

TIGIT/PVR *trans*-Interaction Facilitates Cell-Cluster Formation. One important function of the PVR family of proteins—together with nectins and Necl-proteins—is to promote cell–cell contact by adhesive junction formation. To test if *trans*-heterodimerization of TIGIT and PVR alone would drive cell adhesion, we performed cell–cell adhesion studies using fluorescently labeled BJAB-TIGIT and BJAB-PVR cells (Fig. 4 *A* and *B*). Clustering of cells was monitored with immunofluorescence microscopy and quantified

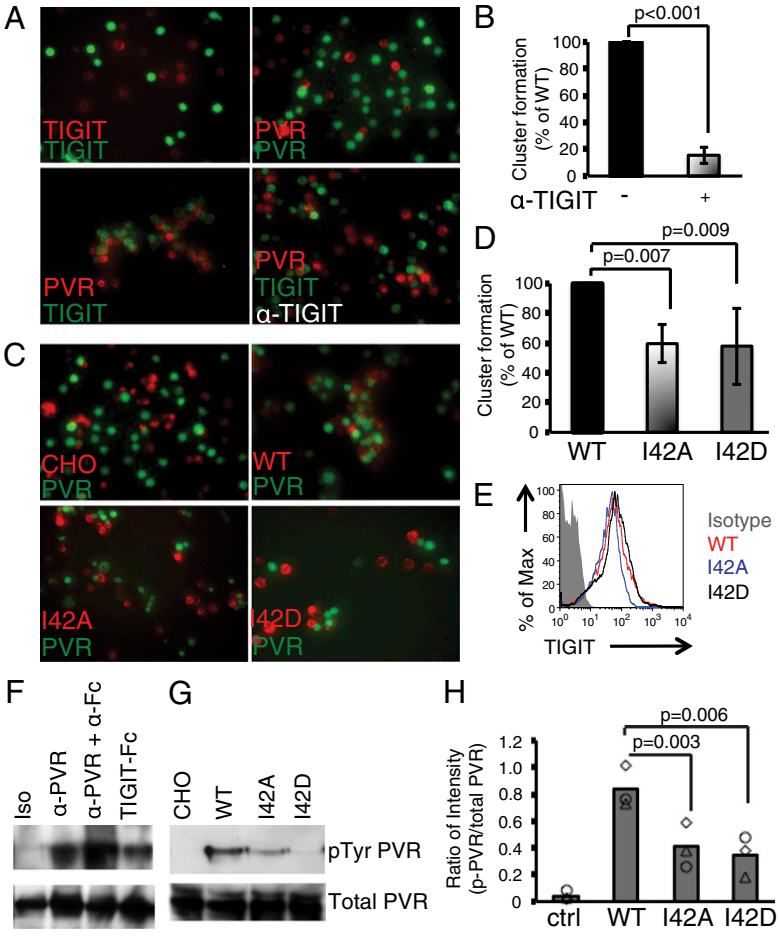

Fig. 4. Lateral TIGIT/TIGIT homodimerization facilitates PVR signaling. (*A* and *B*) Cell-cluster coculture assays performed with stable BJAB cell lines expressing full-length TIGIT or PVR. Cells were labeled with red or green dyes as indicated. (*A*) Representative images of cell clustering (*Upper* panels) of cocultured BJAB cells expressing TIGIT or PVR labeled with PKH26 (red) or CFSE (green) and treated with anti-TIGIT antibody as indicated. (*B*) Quantification of cell-cluster formation for TIGIT-BJAB plus PVR-BJAB cells in the absence or presence of anti-TIGIT antibody by FACS ($n = 3$). (*C* and *D*) Cell-cluster coculture assays performed with stable CHO cell lines expressing full-length TIGIT or TIGIT I42A and TIGIT I42D mutants cocultured with full-length PVR expressed on BJAB cells. (*C*) Representative images of cell clustering by PVR-BJAB cells with CHO alone, TIGIT-CHO, TIGIT-I42A-CHO, or TIGIT-I42D-CHO. (*D*) Quantification of CHO-BJAB cell-cluster formation by FACS ($n = 3$). (*E*) FACS analysis of cell-surface expression, TIGIT WT (red), TIGIT-I42A (blue), and TIGIT-I42D (black) protein on CHO cells. The gray-shaded histogram represents the isotype control. (*F–H*) PVR tyrosine phosphorylation assay with iMDDCs. (*F*) Lysates of iMDDCs—untreated or treated for 5 min at 37 °C with isotype-matched control antibody, anti-PVR, anti-PVR plus anti-IgG, or TIGIT-Fc—were immunoprecipitated with anti-PVR and probed with antibody to phosphorylated tyrosine (α-pTyr; *Upper*) or α-PVR (*Lower*). Results are from one of three independent experiments. (*G*) Human iMDDCs were cultured with CHO, TIGIT-CHO, TIGIT-I42A-CHO, or TIGTI-I42D-CHO cells for 10 min, cell lysates were prepared from isolated iMDDCs, and PVR tyrosine phosphorylation was detected after immunoprecipitation with α-PVR antibody. Representative results from one of three donors are indicated. (*H*) Quantification of the percentage of tyrosine-phosphorylated PVR of total PVR (with film background subtracted) ($n = 3$). Each symbol represents iMMDC from one donor.

by FACS. BJAB-TIGIT or BJAB-PVR cells alone did not aggregate or form cell clusters, suggesting that these individual proteins do not form *trans*-homodimers (Fig. 4*A*, *Upper* panels). However, when cocultured, BJAB-PVR and BJAB-TIGIT formed large cell clusters (Fig. 4*A*, *Lower Left*). The cell clusters were abolished in the presence of the blocking anti-TIGIT (10A7) antibody (4) by 80% (Fig. 4 *A*, *Lower Right* and *B*). Thus, a heterodimer of TIGIT/PVR can mediate cell–cell contacts in culture.

To determine the requirement of TIGIT/TIGIT *cis*-homodimers for cell adhesion and signaling, point mutants of residue Ile42 of TIGIT that are predicted to affect the core dimer interactions were generated and tested for PVR binding. We engineered two point mutations of TIGIT Ile42, I42A and I42D, and expressed the respective full-length proteins in CHO cells. Both CHO-TIGIT-I42A and -I42D bound PVR comparably to wild-type CHO-TIGIT by FACS, suggesting that the mutant proteins were correctly folded; this implied that disruption of the TIGIT dimer interface did not fully inhibit TIGIT/PVR binding (Fig. S7). However, cell clustering was reduced when TIGIT I42A or I42D were used compared with wild-type TIGIT (Fig. 4 *C* and *D*), despite equivalent cell-surface expression (Fig. 4*E* and Fig. S7) and binding of PVR (EC_{50} values for CHO-TIGIT, CHO-TIGIT-I42A, and CHO-TIGIT-I42D were 14.9 μg/mL, 10.9 μg/mL, and 15.7 μg/mL, respectively). Quantification of the cell clusters by FACS showed that both mutants I42A and I42D reduced cluster formation by 30–40% ($P = 0.007$ and $P = 0.009$, respectively). These data suggest that TIGIT *cis*-homodimers are required for robust adhesion to PVR-expressing cells.

Disruption of the TIGIT *cis*-Homodimer Interface Inhibits PVR Signaling. Although the cell-clustering ability of TIGIT/PVR is reduced by destabilizing TIGIT *cis*-homodimers, we asked whether these cell-surface TIGIT *cis*-homodimers were necessary to activate PVR intracellular signaling. PVR is expressed on DCs, and cross-linking with a TIGIT-Fc fusion protein or anti-PVR antibody induces tyrosine phosphorylation of PVR and elicits downstream signaling (4, 22–24). Here we confirmed tyrosine phosphorylation of PVR in human immature monocyte-derived DCs (iMDDCs) after ligation with TIGIT-Fc as well as an agonist anti-PVR mAb, which was further enhanced with Fc cross-linking (Fig. 4*F*). CHO cells expressing TIGIT-WT (CHO-TIGIT) cells could replace TIGIT-Fc protein in this assay in a coculture of iMDDCs with CHO-TIGIT and induced comparable PVR tyrosine phosphorylation (Fig. 4 *G* and *H*). However, PVR tyrosine phosphorylation was significantly decreased using the TIGIT homodimer destabilizing mutants on CHO-TIGIT-I42A or CHO-TIGIT-I42D cells (Fig. 4 *G* and *H*). These results show that TIGIT/PVR *trans*-interaction is necessary for cell–cell adhesion and that robust adhesion to and signaling through its cognate receptor PVR is additionally dependent on TIGIT surface homodimerization.

Discussion

Nectin/Necl homo- and heterodimerization regulates cell adhesion and signaling by the formation of *cis-trans* oligomers on the cell surface of juxtaposed cells. However, the molecular mechanism of this *cis-trans* receptor clustering is currently unknown. Here, we have used the heterodimeric PVR-TIGIT receptor-ligand pair as a model for nectin/Necl *cis-trans* dimerization. We have solved the crystal structures of TIGIT alone and in complex with PVR. The TIGIT/PVR complex structure shows that an interface, common to nectins/Necls and other IgSF homodimers, is necessary for TIGIT/PVR *trans*-heterodimerization. The PVR-TIGIT receptor-ligand pair interacts via three previously described conserved PVR family motifs: (V/I)(S/T)Q, AX_6G, and T(F/Y)P that form a specific lock-and-key interaction. Point mutations in these motifs abrogate complex formation, suggesting high ligand specificity (Fig. 2). All PVR family members share these homologous yet divergent PVR motifs, which might account for the different reported binding affinities (4, 16); we classify the TYP group as TIGIT-like and the TFP group as PVR-like. Thus, the (T/L)YP motif in CD96 and CD226 might interact with PVR in a similar way to TIGIT. Similarly, the TFP motif in nectins fits well into the lock of the TIGIT, CD226, and CD96 molecules. The *trans*-interaction defines how each nectin/Necl binds its receptor partner to form specific cell–cell contacts. The engagement of PVR on DCs with the high-affinity ligand TIGIT induced secretion of the anti-inflammatory cytokines such as IL-10 and TGFβ, which, in turn, attenuated immune responses in vitro and in vivo preclinical models (4).

Surprisingly, the analysis of the TIGIT and TIGIT/PVR crystal structures revealed a tetrameric assembly with a core TIGIT/TIGIT homodimer centered on Ile42 and with converging TIGIT C termini that support the lateral dimerization of TIGIT on the cell surface (Fig. 3). Similar to other noncovalently linked Ig-Ig homodimers (25–27), the affinity of the isolated TIGIT IgV domain is low in solution. Despite the low affinity in solution, we demonstrated that full-length TIGIT is able to form homodimers on the surface of cells. Disruption of the TIGIT *cis*-homodimer interface by a single point mutation at Ile42 did not fully abrogate TIGIT/PVR binding or cell clustering, but TIGIT *cis*-homodimerization was nonetheless essential for PVR activation (Fig. 4) (4, 16). The TIGIT Ile42 mutations support the role of the observed TIGIT homodimer in receptor-ligand clustering conformation in these transfected cells. The TIGIT homodimer is central to the complex, and our data show that it can exist on the cell surface, although we cannot conclude that TIGIT does exist as a homodimer on the cell surface in vivo before ligand engagement.

A similar *cis*-homodimerization mechanism of the PVR D1 domain, and possibly of the PVR D2 domain, suggested by a crystal structure (9) bound in *trans* to a *cis*-homodimer of TIGIT, would likely lead to a tightly packed array of PVR molecules at the immune synapse, enabling an effective receptor clustering and heightening subsequent signaling by tyrosine phosphorylation of the cytosolic PVR ITIM motif. Thus, this work suggests that weaker preformed *cis*-dimers of TIGIT on the cell surface are required for *cis-trans* receptor oligomerization that is necessary for PVR signaling into primary cells. A similar coupling of *cis-trans* dimerization has been investigated for the covalent *cis*-homodimers in the CTLA-4-B7-1/2 complexes and for noncovalent *cis*-homodimers in cadherins as well as in the CAR-JAML complex and the Necl-SynCAM2 (12, 13, 25, 27–30).

The magnitude of T-cell responses is tightly coordinated by immune coreceptors, including those containing ITAM and ITIM intracellular signaling motifs. TIGIT was first identified by searching for genes that are expressed by immune cells and that might function as immunomodulatory receptors on the basis of the protein structure comprising an Ig domain, a transmembrane region, and an ITIM, and PVR was subsequently identified as its high-affinity receptor (4). Beyond documenting this receptor–ligand interaction and defining the PVR family, it was clearly demonstrated that IL-10 induction via PVR is robust enough to inhibit antigen-specific T-cell responses. Additional studies in which the pathway is inhibited—either by blocking proteins or by gene ablation—support the TIGIT-PVR interaction as being important for setting the threshold for T-cell responses in both secondary lymph organs and mucosal sites (31, 32). The predominant immuno-coreceptors on T cells are CTLA-4 and CD28, which engage the same ligands, B7-1 and B7-2, on antigen-presenting cells such as DCs (28, 29, 33); however, additional receptors, such as PD-1 and ICOS, have emerged as important receptors in the immune system to fine-tune T-cell effector functions and maintain T-cell tolerance (34). PVR, together with TIGIT and other PVR-family members, CD226 and CD96, similarly regulate immune responses. Engagement of PVR with TIGIT induces an anti-inflammatory response (4, 31, 32); conversely, PVR interaction with the lower-affinity receptor CD226 on T and NK cells promotes

immune activation (19, 20). This paradigm holds true for a number of paired, homologous ITIM/ITAM receptors on T and NK cells (35) where the inhibiting receptor has a high affinity and the activating receptor has a lower affinity for the shared binding molecule and implies that the activating receptor probably needs to outcompete the inhibiting interaction to convey a signal. The inhibitory receptor CLTA-4 has a higher affinity for the B7 ligands and competes with CD28, the activating receptor, for the shared ligands and thus acts to switch off T-cell activation. Similarly, the inhibitory TIGIT ligand has a higher affinity for PVR than the activating CD226. Thus, the PVR-CD226-CD96-TIGIT activation-inhibition system might function similarly to the CD28-CTLA-4-CD80-CD86 network to control T- and NK-cell responses (33).

Taken together, we propose a model by which PVR signaling relies on a TIGIT-assisted *cis-trans* clustering mechanism of PVR on immune cells (Fig. S8). PVR could form monomers, lateral *cis*-homodimers in the Apo state [similar to other nectin/Necl proteins where *cis*-homodimerization seems to precede *trans*-dimerization by using the same interface (1, 10, 12, 13, 17, 36, 37)], or *cis*-homodimers similar to TIGIT and nectin-1 (9) on one cell (on the left side of Fig. S8). TIGIT could form monomers or preformed dimers on the juxtaposed cell (in the middle of Fig. S8). Cell–cell contact between TIGIT-expressing T cells and PVR-expressing DCs is then formed upon TIGIT/PVR *trans*-interaction (on the right side of Fig. S8). Signaling cluster formation that is necessary for PVR signaling into primary cells is then achieved by *cis-trans* receptor oligomerization. In the absence of *cis*-interactions, cell adhering *trans*-dimers would be formed but no signaling-competent higher-ordered structure would be observed.

In conclusion, our study provides a structural basis for the dual role that PVR provides in cell adhesion and cell signaling via its interaction with TIGIT. Enhanced cell adhesion and signaling of TIGIT into DCs through PVR promote anti-inflammatory cytokines that can dampen an immune response and contribute to the immunological regulation of inflamed tissue and normal homeostatic surveillance. Furthermore, our findings shed light on how nectin/Necl *cis-trans* interactions can organize heterologous cell–cell adhesion and regulate cell signaling.

Materials and Methods

Human TIGIT extracellular domain and human PVR D1 were cloned into pET15b and pACGP67 expression vectors, respectively, and expressed in *E. coli* and in insect cells as described in *SI Materials and Methods*. The individually purified proteins were mixed to form a complex, which was purified further. Detailed methods are outlined in *SI Materials and Methods*. The complex was crystallized in 17% PEG 10000, 0.1 M Bis-Tris (pH 5.5), and 0.1 M ammonium acetate, and diffraction data were collected and processed as described in *SI Materials and Methods*. The structure of the complex was determined by molecular replacement and refined at 2.9 Å to a final R_{work} and R_{free} of 25.0 and 28.4%, respectively. Details of X-ray crystallography methods, BLI, gradient diffusion NMR, analytical ultracentrifugation, TR-FRET, cell aggregation assays, and tyrosine phosphorylation assays are described in *SI Materials and Methods*.

ACKNOWLEDGMENTS. We thank the Baculovirus Expression Unit of the Structural Biology Department at Genentech; Dr. Wayne Fairbrother and Dr. Jacob Corn for critical reading of the manuscript; Dr. Till Maurer for diffusion NMR measurements; and Dr. Barthelemy Demeule for analytical ultracentrifugation experiments. Portions of this research were carried out at the Stanford Synchrotron Radiation Lightsource (SSRL) and the Advanced Light Source (ALS). SSRL is supported by the Department of Energy Office of Biological and Environmental Research; the National Institutes of Health; the National Center for Research Resources, Biomedical Technology Program (P41RR001209); and the National Institute of General Medical Sciences. ALS is supported by the Director, Office of Science, Office of Basic Energy Sciences, of the Department of Energy under Contract DE-AC02-05CH11231.

1. Ikeda W, et al. (2003) Tage4/Nectin-like molecule-5 heterophilically trans-interacts with cell adhesion molecule Nectin-3 and enhances cell migration. *J Biol Chem* 278: 28167–28172.
2. Oda T, Ohka S, Nomoto A (2004) Ligand stimulation of CD155alpha inhibits cell adhesion and enhances cell migration in fibroblasts. *Biochem Biophys Res Commun* 319: 1253–1264.
3. Takai Y, Miyoshi J, Ikeda W, Ogita H (2008) Nectins and nectin-like molecules: Roles in contact inhibition of cell movement and proliferation. *Nat Rev Mol Cell Biol* 9:603–615.
4. Yu X, et al. (2009) The surface protein TIGIT suppresses T cell activation by promoting the generation of mature immunoregulatory dendritic cells. *Nat Immunol* 10(1):48–57.
5. Togashi H, et al. (2011) Nectins establish a checkerboard-like cellular pattern in the auditory epithelium. *Science* 333:1144–1147.
6. Takai Y, Ikeda W, Ogita H, Rikitake Y (2008) The immunoglobulin-like cell adhesion molecule nectin and its associated protein afadin. *Annu Rev Cell Dev Biol* 24:309–342.
7. Aricescu AR, Jones EY (2007) Immunoglobulin superfamily cell adhesion molecules: Zippers and signals. *Curr Opin Cell Biol* 19:543–550.
8. Dong X, et al. (2006) Crystal structure of the V domain of human Nectin-like molecule-1/Syncam3/Tsll1/Igsf4b, a neural tissue-specific immunoglobulin-like cell-cell adhesion molecule. *J Biol Chem* 281:10610–10617.
9. Di Giovine P, et al. (2011) Structure of herpes simplex virus glycoprotein D bound to the human receptor nectin-1. *PLoS Pathog* 7:e1002277.
10. Narita H, et al. (2011) Crystal structure of the cis-dimer of Nectin-1: Implications for the architecture of cell-cell junctions. *J Biol Chem* 286:12659–12669.
11. Zhang P, et al. (2008) Crystal structure of CD155 and electron microscopic studies of its complexes with polioviruses. *Proc Natl Acad Sci USA* 105:18284–18289.
12. Fogel AI, et al. (2010) N-glycosylation at the SynCAM (synaptic cell adhesion molecule) immunoglobulin interface modulates synaptic adhesion. *J Biol Chem* 285:34864–34874.
13. Fogel AI, Stagi M, Perez de Arce K, Biederer T (2011) Lateral assembly of the immunoglobulin protein SynCAM 1 controls its adhesive function and instructs synapse formation. *EMBO J* 30:4728–4738.
14. Mendelsohn CL, Wimmer E, Racaniello VR (1989) Cellular receptor for poliovirus: Molecular cloning, nucleotide sequence, and expression of a new member of the immunoglobulin superfamily. *Cell* 56:855–865.
15. Seth S, et al. (2009) Abundance of follicular helper T cells in Peyer's patches is modulated by CD155. *Eur J Immunol* 39:3160–3170.
16. Stanietsky N, et al. (2009) The interaction of TIGIT with PVR and PVRL2 inhibits human NK cell cytotoxicity. *Proc Natl Acad Sci USA* 106:17858–17863.
17. Mueller S, Wimmer E (2003) Recruitment of nectin-3 to cell-cell junctions through trans-heterophilic interaction with CD155, a vitronectin and poliovirus receptor that localizes to alpha(v)beta3 integrin-containing membrane microdomains. *J Biol Chem* 278:31251–31260.
18. Fujito T, et al. (2005) Inhibition of cell movement and proliferation by cell-cell contact-induced interaction of Necl-5 with nectin-3. *J Cell Biol* 171(1):165–173.
19. Bottino C, et al. (2003) Identification of PVR (CD155) and Nectin-2 (CD112) as cell surface ligands for the human DNAM-1 (CD226) activating molecule. *J Exp Med* 198:557–567.
20. Fuchs A, Cella M, Giurisato E, Shaw AS, Colonna M (2004) Cutting edge: CD96 (tactile) promotes NK cell-target cell adhesion by interacting with the poliovirus receptor (CD155). *J Immunol* 172:3994–3998.
21. Xu Z, Jin B (2010) A novel interface consisting of homologous immunoglobulin superfamily members with multiple functions. *Cell Mol Immunol* 7(1):11–19.
22. Kakunaga S, et al. (2004) Enhancement of serum- and platelet-derived growth factor-induced cell proliferation by Necl-5/Tage4/poliovirus receptor/CD155 through the Ras-Raf-MEK-ERK signaling. *J Biol Chem* 279:36419–36425.
23. Sato T, et al. (2005) Common signaling pathway is used by the trans-interaction of Necl-5/Tage4/PVR/CD155 and nectin, and of nectin and nectin during the formation of cell-cell adhesion. *Cancer Sci* 96:578–589.
24. Coyne CB, Kim KS, Bergelson JM (2007) Poliovirus entry into human brain microvascular cells requires receptor-induced activation of SHP-2. *EMBO J* 26:4016–4028.
25. Verdino P, Witherden DA, Havran WL, Wilson IA (2010) The molecular interaction of CAR and JAML recruits the central cell signal transducer PI3K. *Science* 329:1210–1214.
26. Harrison OJ, et al. (2011) The extracellular architecture of adherens junctions revealed by crystal structures of type I cadherins. *Structure* 19:244–256.
27. Wu Y, Vendome J, Shapiro L, Ben-Shaul A, Honig B (2011) Transforming binding affinities from three dimensions to two with application to cadherin clustering. *Nature* 475:510–513.
28. Stamper CC, et al. (2001) Crystal structure of the B7-1/CTLA-4 complex that inhibits human immune responses. *Nature* 410:608–611.
29. Schwartz JC, Zhang X, Fedorov AA, Nathenson SG, Almo SC (2001) Structural basis for co-stimulation by the human CTLA-4/B7-2 complex. *Nature* 410:604–608.
30. Wu Y, et al. (2010) Cooperativity between trans and cis interactions in cadherin-mediated junction formation. *Proc Natl Acad Sci USA* 107:17592–17597.
31. Levin SD, et al. (2011) Vstm3 is a member of the CD28 family and an important modulator of T-cell function. *Eur J Immunol* 41:902–915.
32. Joller N, et al. (2011) Cutting edge: TIGIT has T cell-intrinsic inhibitory functions. *J Immunol* 186:1338–1342.
33. Alegre ML, Frauwirth KA, Thompson CB (2001) T-cell regulation by CD28 and CTLA-4. *Nat Rev Immunol* 1:220–228.
34. Sharpe AH (2009) Mechanisms of costimulation. *Immunol Rev* 229(1):5–11.
35. Stanietsky N, Mandelboim O (2010) Paired NK cell receptors controlling NK cytotoxicity. *FEBS Lett* 584:4895–4900.
36. Momose Y, et al. (2002) Role of the second immunoglobulin-like loop of nectin in cell-cell adhesion. *Biochem Biophys Res Commun* 293(1):45–49.
37. Yasumi M, Shimizu K, Honda T, Takeuchi M, Takai Y (2003) Role of each immunoglobulin-like loop of nectin for its cell-cell adhesion activity. *Biochem Biophys Res Commun* 302(1):61–66.